18

Conversion of Biogas to Syngas via Catalytic Carbon Dioxide Reforming Reactions: An Overview of Thermodynamic Aspects, Catalytic Design, and Reaction Kinetics

Doan Pham Minh, Ahimee Hernandez Torres, Bruna Rego de Vasconcelos, Tan Ji Siang, and Dai-Viet N. Vo

Abstract

Biogas production has continuously increased worldwide during the last decades. Nowadays, heat, electricity, and biomethane production are the main utilization of biogas at large-scale industrial processes. The research and development on biogas valorization is currently related to synthesis gas production via reforming process, since syngas allows obtaining various chemicals and fuels of high-added value. However, biogas reforming is a complex process, which implies various reactions in parallel, and needs high temperature (>800 °C) to obtain high methane conversion. The development of a highly-performing catalyst, which must be active, selective, thermally stable, and resistant to solid carbon formation on its surface, is crucial. This chapter is devoted to an update of the thermodynamic aspect of biogas reforming under different conditions. This chapter

D. Pham Minh (✉) · A. H. Torres
Université de Toulouse, IMT Mines Albi, Centre RAPSODEE, UMR CNRS 5302, Albi, France
e-mail: doan.phamminh@mines-albi.fr

B. Rego de Vasconcelos
Department of Chemical and Biotechnological Engineering, Université de Sherbrooke, Sherbrooke, Québec, Canada

T. J. Siang
School of Chemical and Energy Engineering, Universiti Teknologi Malaysia, Johor, Malaysia

D.-V. N. Vo
Center of Excellence for Green Energy and Environmental Nanomaterials, Nguyễn Tất Thành University, Hồ Chí Minh City, Vietnam

S. Nanda et al. (eds.), *Biorefinery of Alternative Resources: Targeting Green Fuels and Platform Chemicals*, https://doi.org/10.1007/978-981-15-1804-1_18

also reviews recent significant works related to catalyst design as well as kinetic and mechanistic studies of biogas reforming processes.

Keywords
Biogas · Dry reforming of methane · Tri-reforming of methane · Catalyst · Kinetic study

18.1 Introduction

The green alternatives to fossil fuel have been constantly developed in order to reduce the greenhouse gas emissions. One of the possible solutions is related to biogas, which is considered as a renewable energy source to replace conventional fuels to produce heat, electricity, and chemicals. Biogas is obtained from the decomposition of organic matter under anaerobic conditions (absence of oxygen). The main feedstocks for biogas production include energy crops (e.g., sunflower, wheat grain, sugar beet, etc.), agricultural residues, animal manure, municipal solid waste (MSW), industrial wastes, wastewater, and sewage sludge. These feedstocks contain mostly complex organic compounds, which are degraded by microorganisms under the absence of air through four main steps, such as hydrolysis, acidogenesis, acetogenesis or dehydrogenation and methanation (Jaffrin et al. 2003; Weiland 2010; Mudhoo 2012; Pullen 2015). The hydrolysis of complex polymers into oligomers and monomers (e.g., sugars, amino acids, fatty acids) takes place in the first step. These oligomers and monomers are then degraded into volatile fatty acids ($>C_2$), acetate, and hydrogen. The volatile fatty acids are later converted into acetate, H_2, and CO_2 by acetogenic bacteria. Finally, acetate, H_2, and CO_2 produce CH_4 through methanation. This multi-step transformation needs specific conditions including the absence of air (anaerobic condition), uniform temperature, optimum nutrient supply, optimum and uniform pH (Kaparaju and Rintala 2013).

From the technical point of view, large-scale biogas production can be done in an anaerobic digestion plant or in a landfill site, leading to the formation of digested gas and landfill gas, respectively. The size of these bioreactors varies from some cubic meters to several thousand cubic meters (Persson et al. 2009; Mudhoo 2012; Pullen 2015; Di Maio et al. 2018). Depending on the reactor design, feedstock used, and operational conditions, the composition of biogas can vary. However, biogas typically contains mostly CH_4, CO_2, H_2, N_2, O_2, light hydrocarbons, water vapor, and some pollutants (hydrogen sulfide, ammoniac, siloxanes, and organometallic complexes) (Persson et al. 2009; Pullen 2015; Mudhoo 2012; Kvist and Aryal 2019; Hoo et al. 2018; Eklund et al. 1998; Biogas Renewable Energy 2019). The digested gas generally contains more CH_4 (50–75 vol%) and less CO_2 (30–40 vol%) than landfill gas (CH_4: 35–65 vol% and CO_2: 15–50 vol%). Landfill gas contains varying amounts of N_2 (5–40 vol%) and O_2 (0–5 vol%) while the digested gas generally contains <2 vol% of these gases. This is due to the difficulty of sealing control in landfill sites during landfill gas recovery. Thus, the lower heating value (LHV) of the digested gas (5.5–7.5 kwh/Nm^3) is higher than that of landfill gas (around 4.4 kwh/Nm^3) (Okonkwo et al. 2018; Persson et al. 2009).

Biogas production worldwide continuously increases during the last decades. According to IRENA (2017), the worldwide installed capacity for biogas production increased from 6323 MW in 2007 to 15,752 MW in 2016. Europe represents the highest biogas production capacity with 10,533 MW in 2016 or 66.9% followed by North America with 2639 MW or 16.8% in the same year. In Europe, the top-five biogas producers are, in descending order, Germany, UK, Italy, France, and Netherlands (Achinas et al. 2017). In addition, Scarlat et al. (2018) predicted that biogas production in Europe would still increase with the similar rate during the next years.

Among different feedstocks, MSW is particularly interesting because of its specific characteristics. MSW is generated by households and includes various types of organic and inorganic wastes, which are mostly food waste, waste paper, cardboard, wood, plastic, rubber, and glass. However, it should be noted that the following wastes are not considered as MSW sources, e.g., municipal wastewater sludge, industrial wastes, automobile bodies, combustion ash, or construction and demolition debris. According to Kaza et al. (2018), the worldwide MSW production is predicted to increase from 2.01 billion tons in 2016 to 3.04 billion tons in 2030, mostly due to population explosion and urbanization. MSW composition largely depends on the income of each country. In high-income countries, MSW contains less food waste but more paper and cardboard wastes (from packaging), more rubber and leather (from used tires, clothes, and accessories) compared to low-income, lower-middle, and upper-middle income countries (Kaza et al. 2018). An example of the typical MSW composition in the United States is presented in Table 18.1. The total organic biomass content represents 69.5 wt% illustrating the high potential of biogas generation from MSW.

Up-to-date, the MSW collection is different from each country. In high-income countries, most of the MSW is collected (~100% for both urban and rural zones). This collection rate is lower in other countries, around 85%, 71%, and 45% from urban municipalities in upper-middle, lower-middle, and low-income countries, respectively. In contrast, 45%, 33%, and 26% of MSW are obtained from the rural municipalities in the upper-middle, lower-middle, and low-income countries, respectively. Thus, the effort is still needed for improving MSW collection in these countries. The MSW management by landfill technique is also different from each country. In several developing countries of low and lower-middle income, and

Table 18.1 MSW composition in the United States (Themelis and Ulloa 2007)

Biomass components	Weight %	Petrochemical components	Weight %
Paper/board	36.2	Plastics	11.3
Wood	5.8	Rubber, nylon, etc.	3.7
Yard trimmings	12.1	–	
Food scraps	11.7	–	
Cotton, wool, and leather	3.7	–	
Total biomass	69.5	Total man-made	15

Reprinted from Renewable Energy 32 (2007) 1243–1257, Themelis NJ, Ulloa PA, Methane generation in landfills, pp. 1246, Copyright (2006), with permission from Elsevier

particularly in rural zone, MSW is still burnt in open atmosphere without considering the pollution impacts, technical specification of waste treatment. MSW in some developing countries is treated in open dumping sites without leachate treatment and biogas recovery. In developed countries, sanitary landfill sites are used, which are equipped with lining systems for leachate and biogas recovery, geo-membrane for securing underground water, covering and drainage systems (Youcai and Ziyang 2017). More research is invited to improve the valorization of biogas generated by landfill sites in the world.

18.2 Biogas Utilization and Valorization

18.2.1 Heat and Electricity Production

Biogas mainly contains CH_4 and CO_2 together with other compounds (e.g., water vapor, N_2, O_2, H_2S, NH_3, and siloxanes). One of the primary valorization techniques is the production of heat and electricity. Biogas production in rural areas can be directly used for cooking, household heating, and street lightening without purification or upgrading. This is largely applied in developing countries with the financial incentives by local governments to boost cost-effective waste recycling, local income, and simple utilization (Yasmin and Grundmann 2019; Clemens et al. 2018; Pradhan and Limmeechokchai 2017; Aziz et al. 2019; Khalil et al. 2019; Mittal et al. 2018).

In large-scale urban regions, biogas can be used as a fuel for producing heat and electricity. Biogas utilization is found in the following aspects (Kaparaju and Rintala 2013):

1. Production of heat and/or steam using a boiler.
2. Production of electricity combined with waste heat recovery (combined heat power).
3. Production of heat, steam and/or electricity and cooling using a micro-turbine.
4. Production of electricity using a fuel cell.

It is worth mentioning that raw biogas must be purified before its utilization in an engine to removal pollutants like sulfur-, nitrogen- and chlorine-containing compounds, siloxanes, etc. (Kaparaju and Rintala 2013). In general, the requirement for biogas purification can be classified as follows: fuel cell > gas engine, gas turbine and micro-turbine > stirling engine > boiler (Kaparaju and Rintala 2013).

18.2.2 Biomethane Production

Biogas can also be upgraded into biomethane having the quality of natural gas. This biomethane can be then injected to the gas grid. This valorization way is nowadays commercialized in several countries. The pollutants and CO_2 must be removed from biogas to increase CH_4 content to at least 80 vol% (Elfattah et al. 2016). Different methods are available for biogas upgrading including water scrubbing, chemical scrubbing, biological absorption, pressure swing adsorption, membrane separation,

and cryogenic technology, although each technology has its own advantages and disadvantages (Khan et al. 2017; Sahota et al. 2018; Angelidaki et al. 2018).

Water scrubbing is a simple method with low operation cost and allows CH_4 recovering of more than 80%. However, it requires high energy and water consumption, and has high corrosion risk because of the dissolution of acid gas like hydrogen sulfide. Chemical scrubbing is faster and more efficient, but also more expensive than water scrubbing. Adsorption needs specific operational conditions of pressure, temperature, and adsorbent to reach high efficiency (Pertiwiningrum et al. 2018). According to Angelidaki et al. (2018), the applied commercial technologies for biogas upgrading are as follows: water scrubbing > chemical scrubbing ~ membrane separation > pressure swing adsorption > other technologies. As previously presented, France is in the top-five biogas producers in Europe. The number of biomethane injection stations to the gas grid in France was 37 in June 2017, which has increased to 87 in May 2019 with a total production of 1382 GWh/year (GRDF 2019).

18.2.3 Syngas Production

Synthetic gas (or syngas—a gas mixture rich in CO and H_2) is well known as a versatile platform gas to produce various chemicals and fuels, e.g., methanol, light hydrocarbons, gasoline, diesel, waxes, and alcohols (Brown 2011; Puigjaner 2011; Abdoulmoumine et al. 2015; Liu et al. 2010; Shah 2017; Asimakopoulos et al. 2018; Abdulrasheed et al. 2019). The commercial syngas is produced from fossil resources, e.g., coal, natural gas and heavy hydrocarbons by catalytic steam reforming process (Schildhauer and Biollaz 2016; Liu et al. 2010; Shah 2017). Biogas, mainly containing CH_4 and CO_2, can be used as a renewable feedstock for syngas production.

Syngas production by catalytic steam reforming of biogas has been deployed at large-scale facilities. In the case of the VABHYOGAZ project in France, purified landfill gas was reformed with a molar ratio of steam/water around 4:1 to produce syngas, which is similar to the conditions of natural gas reforming, according to Eq. (18.1). This syngas was later transformed into hydrogen by the water-gas shift process (Grouset and Ridart 2018; Nanda et al. 2017). However, the large excess of steam makes the process highly intensive in energy because the reforming takes place around 900 °C. Current research on biogas reforming into syngas is focused on catalytic dry reforming and tri-reforming processes.

As previously mentioned, biogas mainly contains CH_4 and CO_2. This gas mixture can be transformed into syngas according to Eq. (18.2) which is the chemical reaction of dry reforming of methane (DRM). In this process, CO_2 is the principal oxidizing agent of the reforming of the CH_4 molecule. However, biogas generally contains more CH_4 than CO_2. In addition, water vapor and oxygen are generally present in biogas and can play the role of oxidizing agents in the steam reforming (Eq. 18.1) and partial oxidation (Eq. 18.3) of methane. The combination of three reactions, steam reforming, dry reforming, and partial oxidation of methane constitutes the process of tri-reforming of methane (TRM) (Eq. 18.4) (Table 18.2).

Table 18.2 Methane reforming reactions and side reactions

Reaction	Equation	
Steam reforming	$CH_4 + H_2O \leftrightarrow 3H_2 + CO$ ($\Delta H°_{298}$ = 206.3 kJ/mol)	Eq. (18.1)
Dry reforming	$CH_4 + CO_2 \leftrightarrow 2H_2 + 2CO$ ($\Delta H°_{298}$ = 247 kJ/mol)	Eq. (18.2)
Partial oxidation	$CH_4 + 0.5\ O_2 \leftrightarrow 2H_2 + CO$ ($\Delta H°_{298}$ = − 30.6 kJ/mol)	Eq. (18.3)
Tri-reforming	$xCH_4 + yH_2O + zCO_2 + tO_2 \leftrightarrow uH_2 + vCO$	Eq. (18.4)
Water-gas shift	$CO_2 + H_2 \leftrightarrow CO + H_2O$ ($\Delta H°_{298}$ = 41 kJ/mol)	Eq. (18.5)
Methane cracking	$CH_4 \leftrightarrow C_{(s)} + 2H_2$ ($\Delta H°_{298}$ = 75 kJ/mol)	Eq. (18.6)
Boudouard reaction	$2CO \leftrightarrow C_{(s)} + CO_2$ ($\Delta H°_{298}$ = − 175 kJ/mol)	Eq. (18.7)
Carbon gasification	$C_{(s)} + H_2O \leftrightarrow CO + H_2$ ($\Delta H°_{298}$ = 131 kJ/mol)	Eq. (18.8)
Carbon partial oxidation	$C_{(s)} + 0.5\ O_2 \leftrightarrow CO$ ($\Delta H°_{298}$ = − 110.5 kJ/mol)	Eq. (18.9)
Carbon combustion	$C_{(s)} + O_2 \leftrightarrow CO_2$ ($\Delta H°_{298}$ = − 393.5 kJ/mol)	Eq. (18.10)

Biogas reforming into syngas is accompanied by several side reactions (Eqs. 18.4–18.7), which have an important impact on methane conversion and syngas selectivity as well as catalyst stability. This chapter is focused on the thermodynamic aspects, catalytic design, and reaction kinetics of dry- and tri-reforming of methane. The study of the thermodynamic equilibrium allows determining the limit of a given chemical process under defined conditions of temperature, pressure, and initial composition. The common method of the thermodynamic equilibrium calculation is based on the minimization of Gibbs free energy (Faungnawakij et al. 2007; Nikoo and Amin 2011; Néron et al. 2012).

Nikoo and Amin (2011) have detailed the basis of this method for the dry reforming of methane. Chemical compounds at both gas and solid phases have been considered. The solid considered in this process is related to solid carbon formed during the reaction. The gaseous molecules considered include CH_4, CO_2, CO, H_2, water vapor, methanol, ethylene, ethane, and dimethyl ether (Nikoo and Amin 2011). In the literature, work has been devoted to the thermodynamic study of dry- and tri-reforming of methane (Song and Pan 2004; Faungnawakij et al. 2007; Nikoo and Amin 2011; Jafarbegloo et al. 2015; Abdullah et al. 2017; Pham Minh et al. 2018a, b; Cao et al. 2018; Chein et al. 2017; Chein and Hsu (2018); Rahnama et al. 2014; Diez-Ramirez et al. 2016; Rego de Vasconcelos (2016)). Similar conclusions have been obtained by these studies. This section summarizes the main characteristics of each process.

18.3 Dry Reforming of Methane

For dry reforming of the methane process, Fig. 18.1 shows the amounts of different species in equilibrium from an equimolar mixture of CH_4 and CO_2 (1 mole for each molecule) at 1 and 16 atm. These results were obtained by ASPEN Plus software on the principle of Gibbs free energy minimization described elsewhere (Nikoo and Amin 2011). When the gas mixture is set at 1 atm, solid carbon ($C_{(s)}$) and water vapor are strongly favored below 700 °C. On the other hand, H_2 and CO are predominant above 700 °C. The conversion of CH_4 and CO_2 as well as the selectivity

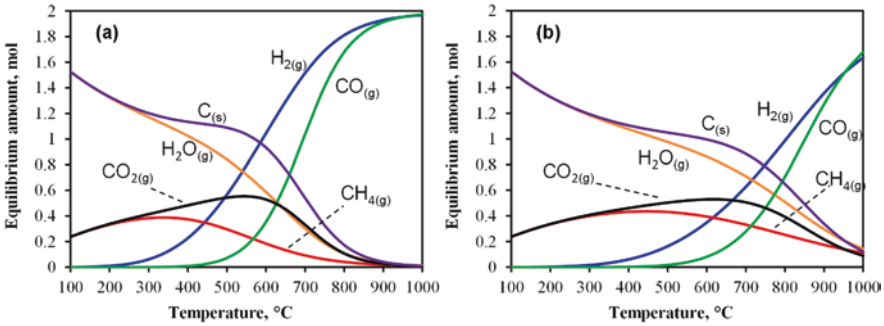

Fig. 18.1 Thermodynamic equilibrium of a gas mixture initially composed of 1 mol of CH_4 and 1 mol of CO_2 at (**a**) 1 atm and (**b**) 16 atm

of H_2 and CO are significantly favored above 900 °C. However, catalyst thermal sintering can occur at this high temperature, which is considered as irreversible catalyst deactivation. Therefore, the design of a thermally stable catalyst is a main challenge of dry reforming of methane. Another characteristic of the dry reforming process is related to solid carbon formation (Eqs. 18.6 and 18.7).

Wang and Lu (1996) have shown that the upper limit of the Boudouard reaction is equal to 700 °C while the lower limit of the methane cracking reaction is equal to 557 °C. Theoretically, there is no temperature range wherein solid carbon formation could be absent. Therefore, dry reforming catalyst must be not only thermally stable but also resistant to solid carbon formation. The formation of solid carbon can be reduced by increasing the molar ratio of CO_2/CH_4. By keeping the temperature at 700 °C and the total pressure at 1 atm, Rego de Vasconcelos (2016) showed that no solid carbon is formed when the molar ratio of CO_2/CH_4 is equal to 2.5/1. However, increasing this ratio also favors the formation of water vapor and slightly decrease the H_2 amount.

Dry reforming of methane produces more gaseous molecules than the initial gaseous reactants (Eq. 18.2). Thus, increasing pressure does not favor this reaction. This decreases CH_4 and CO_2 conversion as well as H_2 and CO selectivity while increases the selectivity in water vapor and solid carbon (Nikoo and Amin 2011; Rego de Vasconcelos 2016; Abdullah et al. 2017; Jafarbegloo et al. 2015). Figure 18.1b illustrates the equilibrium amount of an equimolar mixture of CH_4 and CO_2 when the total pressure is set at 16 atm. At 1000 °C and 16 atm, the unreacted CH_4 and CO_2 amounts are 11.1 and 8.8%, respectively, which are much higher than those at 1000 °C and 1 atm (<1%).

18.4 Tri-reforming of Methane

Tri-reforming process combines steam, dry reforming, and partial oxidation of methane. According to Eq. (18.4), CH_4 can be reformed by varying amounts of water vapor, CO_2, and O_2. Song and Pan (2004) have proposed a concept of

tri-reforming of methane starting from natural gas (CH_4 and CO_2 source) and flue gas (CO_2, O_2, and water vapor) wherein various mixtures of CH_4, CO_2, O_2, and water vapor were considered. Pham Minh et al. (2018a, b) have also simulated various mixtures of landfill gas with water vapor. From the energetic point of view, partial oxidation of methane is exothermal (Eq. 18.3), thus heat from this reaction reduces the energy consumption of the global tri-reforming process (Chein and Hsu 2018). Furthermore, by varying the feeding composition, the molar ratio of H_2/CO can be varied, which is favorable for the downstream application of syngas (Song and Pan 2004). Above 750 °C and at 1 atm, the tri-reforming process generally has higher CH_4 conversion, higher molar ratio of H_2/CO and lower solid carbon amount compared to simple dry or steam reforming (Song and Pan 2004).

Figure 18.2 shows the thermodynamic equilibrium of a mixture initially composed of 2 mol of CH_4, 1 mol of CO_2, 1 mol of water vapor, and 0.1 mol of O_2 at 1 and 16 atm. The sum of oxidizing agents (O_2, CO_2, and water) is in excess for completely converting methane into syngas according to Eq. (18.1–18.3). The composition of this mixture is obtained from the addition of water vapor to a purified landfill gas having the molar ratio of $CH_4/CO_2/O_2$ of 2/1/0.1. At the total pressure of 1 atm, high temperature of at least 800 °C is required to selectively convert this mixture to syngas. Under these conditions, solid carbon could be prevented. In addition, increasing the pressure to 16 bar has negative impacts on reaction conversion and selectivity. At this pressure and 1000 °C, CH_4 conversion only reaches 86.3%.

From the thermodynamic point of view, both dry- and tri-reforming of methane are strongly influenced by the initial feeding composition, temperature, and total pressure. The gas mixture containing more oxidizing agents (e.g., water, CO_2, and O_2) than the stoichiometric amounts favors CH_4 conversion. High temperature also favors CH_4 conversion and syngas selectivity because of the endothermicity of steam and dry reforming of methane. On the other hand, high pressure is unfavorable considering the stoichiometric coefficients of methane reforming reactions.

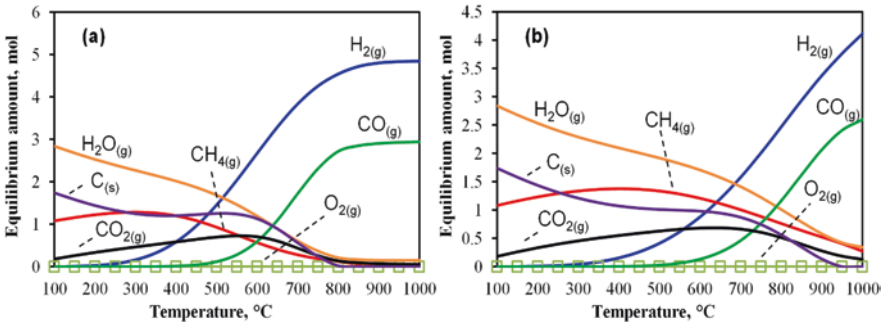

Fig. 18.2 Thermodynamic equilibrium of a gas mixture initially composed of 2 mol of CH_4, 1 mol of CO_2, 1 mol of water vapor, and 0.1 mol of O_2 at (**a**) 1 atm and (**b**) 16 atm

18.5 Catalysts Development

The development of an active and stable catalyst is one of the key points necessary for the implantation of biogas reforming technologies at large-scale operations. Catalyst deactivation related to carbon deposition, sulfur poisoning, and catalyst sintering is one of the biggest issues related to catalytic performance. Therefore, researches have focused on the development of more resistant catalysts using, for example, combination of different active metals, new supports, and promoters. Studies developed through the years on this area have shown that the performance of the catalysts mainly depends on the active metal used on the nature of the support, on the metal-support interaction as well as on other features, such as metal particle size and catalyst surface area. The following topics will discuss the recent advances in catalyst design and application in dry- and tri-reforming of biogas.

18.5.1 Catalysts in Dry Reforming of Methane

Noble metal-based catalysts have been reported as highly active and stable catalysts for dry reforming of biogas with only low amounts of coke formation (Papadopoulou et al. 2012). The main reasons related to the coke resistance of these catalysts are the small equilibrium constants for the decomposition of CH_4 as well as the carbon dissolution into their lattices (Papadopoulou et al. 2012). These findings were reported by Rostrup-Nielsen and Hansen (1993) when they compared the performance of different noble metals catalysts (Ru, Ir, Pd, Pt, and Rh) on dry reforming of methane at temperatures varying between 500 °C and 650 °C. Their results showed that ruthenium (Ru) and rhodium (Rd) had the best catalytic performances with high selectivity for carbon-free operation, thus proving the high coking resistance. Similarly, Hou et al. (2006) evaluated the performance of several noble metals (Ru, Pd, Pt, and Ir) doped on alumina (α-Al_2O_3) catalysts in the dry reforming of methane reaction at 950 °C. The results proved the coking resistance and the stability of these noble metal catalysts with CH_4 and CO_2 conversions higher than 84%. The following order of performance was observed: Rh > Ru > Ir > Pd > Pt. The less efficient performance of the Pd- and Pt-based catalysts was related to the metal particles sintering at high temperature.

Despite the high activity and stability of noble metal-based catalysts, their high cost and low availability render them unattractive for industrial-scale uses. Transition metals have become a suitable alternative due to their low cost, high availability, and good activity in the dry reforming reaction (Pakhare and Spivey 2014). Nickel-based catalysts are often studied since they are already used for advanced reforming process at industrial scale, such as steam reforming (Eq. 18.1). Goula et al. (2015) investigated the performance of Ni/Al_2O_3 catalysts with nickel (Ni) loadings varying between 8 and 16 wt% on the biogas reforming reaction. The authors reported that the catalysts with lower nickel loading exhibited higher specific surface area and low nickel particles than the catalysts with high nickel loadings, which was related to the coverage of the internal surface area by the nickel species adsorbed on

the alumina active sites. However, the authors reported that the nickel loading had no direct effect on the catalytic performance. In this case, the preparation method showed to be the most influencing parameter since it had a direct impact on the reducibility of the nickel species and thus on the overall performance of the catalysts. The 16 wt% Ni/Al_2O_3 catalyst prepared by incipient wetness impregnation method showed the best catalytic performance at 750 °C with CH_4 and CO_2 conversions equaled to 69.1% and 88.3%, respectively.

Despite their low cost and proven catalytic activity, transition metal-based catalysts have been repeatedly reported as more prone to deactivation due to carbon deposition than noble metal-based catalysts (Pakhare and Spivey 2014). Kroll et al. (1997) showed Ni/SiO_2 as a better performing catalyst in the dry reforming reaction at 700 °C showing CH_4 conversion of 93% during the first hours of reaction. However, the catalyst quickly deactivated after less than 10 h of reaction due to carbon deposition. Hence, recent studies have focused on improving the catalytic properties of transition metal-based catalysts.

Bi-metallic catalysts using a combination of two transition metals or between transition metals and noble metals have been tested to improve the catalytic properties of the catalysts. Among the various combinations of transition metals used, nickel (Ni) and cobalt (Co) are by far the most investigated combination due to the synergy between these two metals as well as to the property of cobalt of decreasing the rate of coke formation (Estephane et al. 2015). The influence of cobalt addition to the performance of Ni/ZSM5 catalyst on dry reforming reaction at temperatures ranging from 600 °C to 800 °C was investigated by Estephane et al. (2015). The authors suggested that the cobalt presence could help oxidizing the carbon species close to the catalytic sites, thus increasing the stability of the catalyst. The best catalytic result was obtained using a Ni/Co ratio equal to 1:2. This catalyst exhibited CH_4 and CO_2 conversion equal to 80% and 85%, respectively, at 800 °C, proving the good catalytic performance of this bi-metallic catalyst.

Similar results were achieved by Xu et al. (2009). The addition of cobalt significantly increased the catalytic performance of the Ni/La_2O_3-Al_2O_3 catalyst. The authors reported CH_4 and CO_2 conversions equal to 93.7% and 94%, respectively, in biogas reforming at 800 °C and 290 h when a bi-metallic catalyst with a Ni/Co molar ratio equal to 7:3 was used. Besides carbon deposition, sulfur poisoning also leads to catalyst deactivation during biogas reforming. Recent studies have shown that the use of bi-metallic catalysts could improve the sulfur resistance of the catalysts. Sapountzi et al. (2018) showed that doping Ni/GDC (gadolinia-doped ceria) catalyst with 2.3 wt% of gold (Au) hindered the formation of strongly bonded sulfur components by producing an Au-Ni alloy.

The textural and chemical promoters have also been used to improve the catalytic performance of the catalysts. According to Jang et al. (2019), promoters are usually used to enhance the textural properties of the catalysts, which helps preventing or delaying sintering of the active phase. Chemical promoters provide new active sites or enhance chemical properties, such as basicity and redox property, which prevent carbon formation (Jang et al. 2019). San José-Alonso et al. (2011) investigated the use of potassium (K) and strontium (Sr) on the performance of Co/Al_2O_3 on CO_2 reforming

of CH_4 at 700 °C. The authors reported that the Co/Al_2O_3 catalyst showed CH_4 and CO_2 conversions of 73% and 82%, respectively. The percentage of deposited carbon was 0.53%. When this catalyst was doped with 1 wt% K or 1 wt% Sr, CH_4 and CO_2 conversions decreased to about 15%. The percentage of deposited carbon also decreased, achieving 0.08% when K was used. The main reason for the decrease in the CH_4 conversion was related to the partial coverage of the active sites for CH_4 decomposition and to the ability of the catalyst to gasify the carbon species.

Ceria (Ce) has also been reported to improve the coke resistance of the catalysts. Daza et al. (2010) investigated the effect of Ce addition and loading on Ni/Mg-Al catalyst on dry reforming at 700 °C. The addition of 1 wt% of Ce to the catalyst was responsible for increasing CH_4 conversion from 34.9% to 88.3%. The authors reported that Ce addition increased the reducibility and the total basicity of the catalyst, which was responsible for the increase in the catalytic activity. However, increasing Ce content from 1 to 10 wt% did not have an influence on the catalyst activity but it greatly hindered the formation of coke deposits. The catalyst doped with Ce was stable in the reaction conditions during 100 h of reaction.

18.5.2 Catalysts in Tri-reforming of Methane

As presented in the previous sections, tri-reforming is a synergetic combination between dry reforming, steam reforming, and partial oxidation. Hence, it is not surprising that the catalytic systems used in the tri-reforming process are similar to those used in the other advanced reforming process and face similar problems, such as low stability due to coke deposition and metal sintering. However, the tri-reforming process is a much more complex process due to the presence of three oxidizing agents (e.g., O_2, CO_2, and H_2O), requiring a catalyst capable of adsorbing and activating all three reactants efficiently as well as to withstand the highly oxidizing atmosphere. The following topics will briefly present the recent advances in catalyst development for this process as well as the efforts for scaling up the technology.

Nickel supported on conventional catalytic supports, such as Al_2O_3, ZrO_2, SiO_2, and CeO_2 is the most studied active metal. However, these catalysts may behave differently in tri-reforming conditions mainly due to their re-oxidation by the oxygen in the feed, which leads to their deactivation (Amin et al. 2015). Majewski and Wood (2014) investigated the performance of Ni/SiO_2 core shell catalyst in steam reforming of methane in tri-reforming conditions at 750 °C. The authors reported that changing the percentage of each oxidizing agent (O_2, CO_2, and H_2O) in the feed mixture had a different impact on the performance of the catalyst. Increasing the amount of oxygen in the feed mixture increased the CH_4 conversion to 90% but did not improve the H_2/CO ratio in the produced syngas. When steam was not present in the feed, CO_2 conversion increased to 90%, but CH_4 conversion decreased. When steam was added with a CH_4/H_2O ratio of 1:0.5, the H_2/CO ratio of the syngas decreased from 2.5 to 1.5 and coke deposition increased from 5 mg g_{cat}^{-1} up to 99 mg g_{cat}^{-1}. These results show the potential of Ni/SiO_2 core-shell catalyst in the tri-reforming process. However, it also highlights the complexity to maintain high reactants' conversion and good catalyst stability.

The role of the support in tri-reforming is also not yet defined and further studies to correlate the physicochemical properties of the catalysts to their performance are still needed. Different supports have been used to prepare catalysts for tri-reforming reaction, including CeO_2 (Pino et al. 2011), TiO_2 (Jiang et al. 2007), ZrO_2 (Si et al. 2012; Singha et al. 2016; Anchieta et al. 2019), $MgAl_2O_4$ (Lino et al. 2019), and SiC (García-Vargas et al. 2014a, 2014b, 2015b). In attempt to investigate the influence of different support materials on the performance of nickel-based catalysts, Kumar et al. (2019) prepared different catalysts using Al_2O_3, ZrO_2, MgO, CeO_2-ZrO_2, SBA-15, and TiO_2 as the supports and evaluated their performance in tri-reforming at 800 °C and with a feed composition of CH_4/CO_2/H_2O/O_2/N_2 of 1:0.23:0.46:0.07:0.28. The authors reported that Ni/Al_2O_3 had the best catalytic performance in the test conditions used with CH_4, H_2O, and CO_2 conversion rates equal to 8.72×10^{-1} mmol g_{cat}^{-1} s, 4.2×10^{-2} mmol g_{cat}^{-1} s, and 2.31×10^{-2} mmol g_{cat}^{-1} s, respectively. However, Ni/CeO_2-ZrO_2 and Ni/ZrO_2 showed better stability against oxidation, due to their redox and oxophilic properties, respectively. On the other hand, Ni/MgO and Ni/TiO_2 catalysts showed only very low CH_4 and CO_2 conversion rates since they presented a very low degree of reducibility. The authors concluded that small Ni particles with high dispersion, high degree of reducibility, strong metal-support interaction as well as high concentration of basic sites on the surface of the catalyst are crucial for the good catalytic performance of the catalysts.

García-Vargas et al. (2014b) investigated the performance of Ni/Al_2O_3 and Ni/CeO_2 catalysts in tri-reforming conditions at 800 °C. The best catalytic result was obtained using Ni/CeO_2 catalyst, showing CH_4 and CO_2 consumption rates around 8 and 3 mol s^{-1} g_{Ni}^{-1}, respectively, which was explained by its basic properties. Ni/Al_2O_3 showed the lowest CH_4 and CO_2 conversion rates due to the formation of $NiAl_2O_4$ phase, thus decreasing the reducibility of the catalyst. Pino et al. (2011) have found that Ni/CeO_2 (5 wt%) catalysts prepared by flaming combustion at 350 °C were highly active and selective in tri-reforming of methane at 800 °C with methane conversion up to 93%. The addition of La slightly increased the catalytic performance of these catalysts.

Singha et al. (2016) investigated Ni/ZrO_2 catalysts synthesized by hydrothermal method in the reforming of different mixtures containing CH_4, CO_2, water vapor, and oxygen at 500–800 °C. In most of the case, CH_4 conversion likely linearly increased with the reaction temperature while the molar ratio of H_2/CO varied in narrow range of 1.7–2.0. The optimal Ni content was found at 4.8 wt%, explained by the dependency of Ni particle size on Ni content. At 800 °C, this catalyst was found very active and stable with reactants' conversion close to 96–98% for 100 h of reaction time. This catalytic performance was mostly explained by the formation of metal nanoparticles strongly interacted with the support.

During the last decade, much work has been devoted to the design of a performing catalyst for biogas reforming, e.g., dry- and tri-reforming. Nickel has been found as the most appropriate active metal for these processes. Such a catalyst is generally constituted of (a) a thermally stable support at 700–1000 °C, (b) highly dispersed metal particles (<40 nm), (c) strong metal-support interaction,

and (d) controlled basicity. The addition of promoters could also improve catalyst performance. Despite encouraging results, large pilot application of dry- and tri-reforming is still limited.

18.5.3 Catalyst Supports

Besides the active metal and promoters, the nature of the support also plays a significant role in the performance of the catalysts. Catalyst supports provide mechanical and thermal stability to the catalysts and confer high specific surface area, leading to high metal dispersion, which favors the CH_4 adsorption and dissociation (Papadopoulou et al. 2012). Moreover, strong metal-support interaction is responsible for the high stability of the metal particles during the reaction, which will prevent sintering and coking (Jang et al. 2019). Other support features, such as basic-acid characteristics and oxygen storage capacity also play an important role in the overall performance of the catalysts (Mohamedali et al. 2018).

Al_2O_3 is one of the support materials most used for reforming applications due to its low cost and high mechanical and thermal stability (Papadopoulou et al. 2012). Mo et al. (2015) recently investigated the application of Ni/Al_2O_3 porous catalysts in dry reforming of CH_4. The catalyst synthesized by hydrolysis-deposition method had high specific surface area of 477 m^2/g and small nickel particles of about 7 nm, which ensured high CH_4 and CO_2 conversions of around 95% during 10 h of time on stream. However, depending on the synthesis method used, large metal particles (>10 nm) or even phases difficult to reduce, such as nickel aluminate can be formed, thus decreasing the performance of the catalyst. The acid sites present in this support rendered the alumina-based catalysts more prone to deactivation by carbon deposition.

Hydrotalcite-like materials containing aluminum (Al) and magnesium (Mg) have been intensively investigated for dry reforming applications mainly due to their basic character, which improve coke gasification to their high surface area and to the presence of di and trivalent cations that leads to a homogeneous distribution of the active phase in the matrix (Dębek et al. 2015). de Vasconcelos et al. (2018a) recently investigated the performance of MgAl hydrotalcite-based catalysts doped with Ni and with MgO loads varying from 0 wt% to 70 wt% in the dry reforming reaction at 700 °C. The authors reported that the catalyst with an MgO loading of 70 wt% presented the best catalytic performance with CH_4 and CO_2 conversions around 80% during 50 h of time on stream as well as the lowest deactivation rate of about 0.004% h^{-1}. The catalytic performance of this catalyst was related to the presence of strong basic sites that favored the carbon gasification during the reaction. Moreover, a NiO-MgO solid solution was formed, which stabilized the active phase and prevented its sintering.

Rare earth-based supports, specially ceria, have been also been studied due to its ability to enhance the availability of hydroxyl (OH_{ads}) and surface oxygen (O_{ads}) species, which controls the formation of carbon deposits (Papadopoulou et al. 2012). Wolfbeisser et al. (2016) studied the dry reforming reaction over ceria-zirconia-supported Ni

catalysts at 600 °C. The authors reported that the presence of Ce did not improve the catalytic stability of the catalyst. However, it considerably increased its stability but hindering the formation of filamentous coke. The authors further reported that the influence of ceria strongly depends on the catalyst synthesis method, which can affect the presence of surface oxygen species and of oxygen vacancies. These factors are crucial for the carbon removal at the metal/support surface.

Ceria/zirconia-based supports have been investigated by many authors (Djinovic et al. 2012, 2015; Aw et al. 2014a, b, 2015; Djinovic and Pintar 2017). Solid solutions of ceria/zirconia with high specific surface area, high oxygen storage capacity, and high interaction with nanoparticles of nickel and cobalt as active metals have been found as the main factors responsible for high catalytic performance in dry reforming of methane. These catalysts strongly limited the formation of coke during dry reforming reaction. However, water has been usually found as byproduct with high selectivity (up to 20% in the gas mixture at the reactor outlet) (Aw et al. 2015), suggesting that the designed catalyst favors reversed water-gas shift reaction.

Finally, hydroxyapatite (HAP, chemical formula: $Ca_{10}(PO_4)_6(OH)_2$) has also been found as a new promising catalyst support for the dry reforming of methane (Boukha et al. 2007, 2019; de Vasconcelos 2016; de Vasconcelos et al. 2018a, c; Phan et al. 2018). Hydroxyapatite-supported metals catalysts (e.g., Pt, Ni, and Co) have been found active, selective, and stable in dry reforming reactions and are competitive compared to catalysts prepared from conventional supports like Al_2O_3 and $MgAl_2O_4$ (de Vasconcelos et al. 2018a). The performance of hydroxyapatite in this reaction could be explained by a high thermal stability, a controlled acido-basicity via the molar ratio of Ca/P, and a good cation exchange capacity allowing a strong support-metal interaction between metal nanoparticles and hydroxyapatite surface (de Vasconcelos 2016; Boukha et al. 2019).

18.6 Kinetic Models and Mechanism Aspects

In this section, an overview of reaction mechanisms and kinetics for dry- and tri-reforming of methane are systematically discussed. Understanding the inherently catalytic mechanisms and establishing comprehensive kinetic models for precisely predicting the consumption and formation rates of the corresponding reactants and products are crucial for catalyst design, process optimization, and reactor fabrication and scale-up.

18.6.1 Kinetics of Dry Reforming of Methane

Dry reforming of methane is widely known as a highly endothermic reaction, which is thermodynamically favored at high reaction temperature (Aramouni et al. 2018). However, at such high reaction temperature, dry reforming is also accompanied by several parallel side reactions such as CH_4 decomposition, which provoke carbonaceous deposits leading to catalytic deactivation (Pakhare and Spivey 2014;

Kawi et al. 2015; Bian et al. 2017). Therefore, the understanding of fundamental dry reforming mechanism is crucial for kinetically resisting carbonaceous formation and simultaneously enhancing syngas yield as well as H_2 selectivity. Generally, the mechanistic pathways for syngas production from dry reforming of methane can be summarized into four major mechanisms, such as: (a) dissociative CH_4 adsorption, (b) dissociative CO_2 adsorption, (c) formation of hydroxyl groups, and (d) oxidation and desorption of intermediate species. The comprehensive review for these main dry reforming mechanisms is provided as follows:

1. Dissociative CH_4 adsorption: The dissociation energy for CH_x-H bonds in CH_4 reactant on the catalyst surface is mainly reliant on the intrinsic attributes of active phases and CH_4 dissociation step is widely recognized as the rate-determining step in dry reforming of methane (Tang et al. 2014; Horn and Schlögl 2015). In particular, CH_3 species are adsorbed on the top of active metal atoms, whereas CH_2 species are adsorbed in the middle of two active metal atoms also referred as bridged adsorption (Tang et al. 2014).
2. Dissociative CO_2 adsorption: CO_2 adsorption and dissociation are dependent on surface structure and structural defects of catalysts (Aramouni et al. 2018). In fact, this process can occur through three routes including C-only coordination, O-only coordination (in which an active metal surface is bonded with two O-atoms), as well as C and O coordination (wherein C and O atoms are adsorbed on catalyst surface meanwhile another O atom is left to expose) (Papadopoulou et al. 2012; Guharoy et al. 2018).
3. Formation of hydroxyl groups: Numerous dry reforming kinetic studies reveal that the water-gas shift (WGS) reaction nearly reaches equilibrium, indicating the rapid rate of associated surface reaction. The adsorbed H species from H_2 spillover on active metal surface reportedly migrate to support and subsequently react with adsorbed O-species to form hydroxyl groups. However, this process is unfavorable at high temperature beyond 800 °C (Papadopoulou et al. 2012; Bobadilla et al. 2017).
4. Oxidation and desorption of intermediates: The adsorbed CH_x species on active sites, denoted as S-CH_x, could react with surface oxygen leading to the formation of S-CH_xO and/or S-CO groups. Several proposed pathways for CO formation reportedly include the generation of intermediate S-CH_xO species and reduction of carbonates (formed by adsorbed CO_2) by surface carbon species. In general, the formation and/or decomposition of S-CH_xO species to H_2 and CO gases are recognized as the rate-determining step (Papadopoulou et al. 2012; Jiang et al. 2017; Das et al. 2018).

In general, the kinetic models typically employed in dry reforming of methane can be mainly categorized into empirical power law, Langmuir Hinshelwood-Hougen Watson (LHHW), and Eley Rideal (ER) models. Amongst these kinetic models, the practical and most simple power law model, as provided in Eq. (18.11), is commonly used since it is regarded as one of the easiest computational models for estimating the pertinent reaction parameters.

$$-r_{CH_4} = kP_{CH_4}^{m} P_{CO_2}^{n} \tag{18.11}$$

where k and P_i (i: CO_2 or CH_4) are the corresponding apparent rate constant of CH_4 and partial pressure of reactants, while m and n represent the reaction orders for the corresponding CH_4 and CO_2 reactants, and $-r_{CH4}$ is the CH_4 reaction rate.

The simplicity of power law model, which does not require the full understanding of elementary dry reforming reaction steps since this model is not derived from mechanistic pathways has made it to be extensively employed in many studies for approximate kinetic parameters estimation. As the power law model is not based on the surface mechanism of dry reforming of methane, this model is slightly inaccurate and inappropriate for the investigation of wide-ranging feedstock compositions in comparison with other mechanism-based kinetic models. Nevertheless, this empirical model is advantageous for providing an initial guess of reactants' power constants and apparent activation energy, E_a (kJ mol^{-1}). These useful parameters can be used for the justification of catalytic activity and comparison purpose among reported catalysts in literature.

Table 18.3 lists the computed reaction orders of CH_4 and CO_2 reactants and CH_4 activation energy obtained via power law model for numerous catalysts in recent dry reforming studies. Ayodele et al. (2016) found that CH_4 and CO_2 reaction orders were 3.66 and 0.35, respectively, with the apparent CH_4 activation energy of 96.4 kJ/mol on the La_2O_3-supported cobalt catalyst in dry reforming of methane. The higher CH_4 reaction order than that of CO_2 could indicate the larger dependence on CH_4 partial pressure for CH_4 dissociative adsorption. In addition, they found that the great oxygen storage capacity of La_2O_3 support supplied mobile lattice oxygen to enhance coke gasification from the catalyst surface. This evolution reasonably explains the low CH_4 activation energy (96.4 kJ/mol) on Co/La_2O_3 compared to other catalysts such as Pt/ZrO_2 (Wei and Iglesia 2004) and Ni/α-Al_2O_3 (Cui et al. 2007) with E_a of 100.56 and 106.84 kJ/mol, correspondingly.

In the kinetic study of dry reforming of methane over $SmCoO_3$ perovskite catalyst, Osazuwa et al. (2017) found similar activation energy values for CH_4 and H_2 whereas CO_2 activation energy was reportedly close to that of CO. Thus, they suggested that H_2 and CO formation rates were mainly affected by the corresponding CH_4 and CO_2 consumption rates. Karam and Hassan (2018) used SBA-15 supported Ni catalysts for dry reforming of methane and found that the activation energies of reactants (e.g., CH_4 and CO_2) were smaller than those of products (e.g., H_2 and CO), indicating that the formations of H_2 and CO via surface reaction between adsorbed species are the rate-determining step.

As previously mentioned, the empirical power law models cannot elucidate the involvement of inherent elementary steps on surface reaction during dry reforming of methane since these models are mainly reliant on statistical criteria and could yield untrue kinetic parameter values. Hence, ER and LHHW models are broadly implemented to capture reactant consumption rates and product distribution in dry reforming as they are derived from the intrinsic mechanistic reaction steps. In the dry reforming study of Ru or Pt loaded TiO_2, Singh and Madras (2016) found that the typical peaks belonging to CO_2 adsorption were not detected but CO_2 in the gas

Table 18.3 Kinetic parameters obtained via power law models for dry reforming on various catalysts

Catalyst	Temperature (°C)	Apparent CH_4 activation energy, E_a (kJ/Mol)	Reaction order		References
			m	*n*	
		CH_4	CH_4	CO_2	
Co/La_2O_3	650–750	96.4	3.66	0.35	Ayodele et al. (2016)
Ir-Ni/SBA-15	580–620	26.4	1.54	0.69	Karam and Hassan (2018)
Ni/SBA-15	580–620	35.1	0.99	0.97	Karam and Hassan (2018)
$Ni_{0.07}Mg_{0.93}O$	500–700	84.0	1	–	Zhou et al. (2018)
$Ru_{0.003}Ni_{0.067}Mg_{0.93}O$	500–700	92.0	1	–	Zhou et al. (2018)
$Ru_{0.07}Mg_{0.93}O$	500–700	74.0	1	–	Zhou et al. (2018)
$SmCoO_3$	700–800	41.0	1.15	0.33	Osazuwa et al. (2017)

Table 18.4 Representatives of LHHW and ER kinetic expressions for dry reforming of methane

Catalyst	Assumption	Mechanistic pathways	Kinetic model	Eq. No.	Refs.
Pt/TiO_2	Molecularly adsorbed CH_4 with the dissociation of CH_4 as RDS	$CH_4 + S^* \overset{K_1}{\leftrightarrow} CH_4 - S$ $CH_4 - S \overset{k_2}{\rightarrow} 2H_2 + C - S(RDS^*)$ $C - S + CO_2 + S \overset{K_3}{\leftrightarrow} 2CO - S$ $2CO - S \overset{K_4}{\leftrightarrow} 2S + 2CO$	$-r_{CH_4} = \frac{k_2 K_1 K_3 K_4 P_{CO_2} P_{CH_4}}{K_3\sqrt{K_4} P_{CO} + P_{CO}^2 + \left(1 + K_1 P_{CH_4}\right) K_3 K_4 P_{CO_2}}$	(18.12)	Singh and Madras (2016)
NiCeMgAl	CO_2 and CH_4 dissociative adsorption and the removal of adsorbed C species by adsorbed OH as RDS	$CH_4 + S \overset{K_1}{\leftrightarrow} CH_4 - S$ $CH_4 - S + 4S \overset{K_2}{\leftrightarrow} C - S + 4H - S$ $CO_2 + S \overset{K_3}{\leftrightarrow} CO_2 - S$ $CO_2 - S + H - S \overset{K_4}{\leftrightarrow} CO - S + OH - S$ $C - S + OH - S \overset{k_5}{\rightarrow} CO - S + H - S(RDS)$ $2H - S \overset{K_6}{\leftrightarrow} H_2 + 2S$ $CO - S \overset{K_7}{\leftrightarrow} CO + S$	$-r_{CH_4} = k_5 \frac{K_1^4 K_2^4 K_3^4 K_4^4 K_6^4 K_7^4 P_{CH_4}^4 P_{CO_2}^4}{P_{CO_2}^4 P_{H_2}^6} \left(\frac{C_1}{DEN}\right)^8$ $DEN = 1 + K_1 P_{CH_4} + \frac{K_1 K_2 K_6^2 P_{CH_4}}{P_{H_2}^2} + \frac{P_{H_2}^{0.5}}{K_6^{0.5}} + K_3 P_{CO_2} + \frac{P_{CO}}{K_7} + \frac{K_3 K_4 K_7 P_{CO_2} P_{H_2}^{0.5}}{K_6^{0.5} P_{CO}}$	(18.13)	Bao et al. (2017)

$La_2RhZr_2O_7$	CO_2 and CH_4 dissociative adsorption and CH_4 dissociation as RDS	$CH_4 + S \overset{K_1}{\leftrightarrow} CH_4 - S$ $CH_4 - S \overset{k_2}{\rightarrow} C - S + 2H_2\,(\mathrm{RDS})$ $CO_2 + S \overset{K_3}{\leftrightarrow} CO_2 - S$ $CO_2 - S \overset{K_4}{\leftrightarrow} O - S + CO$ $H_2 + O - S \overset{K_5}{\leftrightarrow} S + H_2O$ $C - S + H_2O \overset{K_6}{\leftrightarrow} S + CO + H_2$	$-r_{CH_4} = \frac{k_2}{K_1} P_{CH_4} \left(1 + K_1 P_{CH_4}\right) \frac{K_4 P_{CO} P_{H_2}}{K_3 K_5 K_6 P_{CO} P_{H_2} P_{CO_2}}$	(18.14)	Pakhare et al. (2014)

*S and RDS represent the corresponding active site and the rate-determining step, whereas C_t is the total number of active sites

phase was observed in in-situ Fourier transform infrared spectroscopy (FTIR) studies. In addition, adsorbed CH_4 species on catalyst surface were evidenced suggesting that dry reforming of methane over the abovementioned catalysts followed the ER mechanism. Thus, an ER kinetic model was proposed with the assumption of molecularly adsorbed CH_4 on active site and the subsequent CH_4 dissociation as the rate-determining step as shown in Eq. (18.12) of Table 18.4. The dissociated carbon species were further reacted with CO_2 in the gas phase to yield CO gas. This derived ER model demonstrated an excellent validation with experimental data.

Bao et al. (2017) examined NiCeMgAl catalyst for dry reforming of methane and developed an LHHW kinetic model (Eq. 18.13 in Table 18.4) based on the assumption of irreversibly adsorbed carbon gasification by surface –OH species as a rate-determining step and consideration of the significant contribution of the reverse water-gas shift reaction. Both CO_2 and CH_4 reactants were also assumed to adsorb dissociatively on the same active site of catalyst. The fitting of CH_4 consumption rate data to the derived kinetic model showed a high correlation coefficient of 0.97, indicative of satisfactory projection for dry reforming reaction rate.

In the kinetic and mechanistic studies of dry reforming of methane over $La_2RhZr_2O_7$ pyrochlores, Pakhare et al. (2014) conducted the deuterium kinetic isotope experiments with the employment of CD_4 during dry reforming and revealed that the rate-determining step was CH_4 activation or dissociation on active sites. Hence, an LHHW model involving dissociative CH_4 adsorption as a rate-determining step (Eq. 18.14 in Table 18.4) was proposed and in line with the obtained experimental data of kinetic and transient pulsing measurements.

18.6.2 Kinetics of Tri-reforming of Methane

Tri-reforming of methane is typically a synergistic combination of multiple reactions involving steam reforming of methane (SRM), dry reforming of methane, and partial oxidation of CH_4 (Song and Pan 2004). However, the kinetic and mechanistic studies of tri-reforming of methane are comparatively less than other reforming reactions owing to its complexity with the highest number of concomitant side reactions. Thus, mechanistic and kinetic investigation of tri-reforming of methane would turn out to be a crucial and alluring research area in the coming years.

The fundamental understanding of mechanism-derived kinetics is still vague and fewer studies have been carried out for tri-reforming of methane. Song and Pan (2004) conducted the first kinetic study of tri-reforming of methane over Ni-based catalysts. To identify the varied CO_2 conversion rate associated with reactant partial pressures, an empirical power rate law (Eq. 18.15) was simplified by retaining the CH_4 and O_2 partial pressures as constants. Therefore, the contribution of CH_4 and O_2 partial pressures would be reflected by other model parameters:

$$-r_i = A_{exp}\left(\frac{-E_{app}}{RT}\right)P_{CO_2}^{\alpha}P_{H_2O}^{\beta} \tag{18.15}$$

where $-r_i$, E_{app}, and A are the corresponding CH_4 or CO_2 reaction rates, apparent activation energy, and pre-exponential factor. P_{H2O} and P_{CO2} are the partial pressure of H_2O and CO_2 reactants, whereas α and β are reaction orders belonging to CO_2 and H_2O, respectively. The computed values of kinetic parameters obtained from Eq. (18.15) for tri-reforming of methane over different Ni-based catalysts are summarized in Table 18.5. From the experimental data and computational results, Song and Pan (2004) observed the negative reaction order values for H_2O reactant during the fitting of CO_2 consumption rates to the abovementioned power law model (Eq. 18.15) for all catalysts. This observation indicated the competitive adsorption between H_2O and CO_2 on the catalyst surface for reacting with CH_4 to yield H_2 and CO. As a result, an increase in P_{H2O} reasonably reduced the rate of CO_2 consumption. As seen in Table 18.5, reaction orders also varied considerably depending on catalysts employed.

To intrinsically scrutinize the interaction between catalyst surface and CO_2 molecule with respect to mechanistic steps, they also employed a simplified LHHW model, which was derived from dry reforming side reaction for minimizing the intricacy of tri-reforming of methane. These mechanistic steps including the adsorption of CH_4 and CO_2 reactants as well as surface reaction are provided in Table 18.6. As seen in the simplified kinetic model, the interaction between catalyst surface and CO_2 molecules was the major factor accounting for the equilibrium CO_2 adsorption constant, i.e., K_2. The enhancing interaction of CO_2 with catalyst surface would provoke an increase in the number of adsorbed CO_2 species at high P_{CO2}. Hence, these adsorbed CO_2 species occupied most of active sites available for CH_4 adsorption, thereby inducing a drop in CH_4 consumption rate. This could be indicative of negative CO_2 reaction order.

In the assessment of Ni-Mg/β-SiC at varied temperature and reactant feed ratios for tri-reforming of methane, García-Vargas et al. (2015b) observed that methane partial oxidation with the rapid achievement of full conversion was the predominant process among other concomitant main reactions since oxygen reactant was virtually absent in gaseous effluent from tri-reforming of methane. Based on this observation, a kinetic model merely in association with steam reforming, dry reforming, and water-gas shift reaction was proposed for capturing the individual rate of these reactions (see Table 18.7). The apparent activation energy of steam reforming, dry

Table 18.5 Kinetic parameters obtained from simplified power law model for tri-reforming of methane by Song and Pan (2004)

Kinetic parameters	Ni/Al_2O_3	Ni/MgO	Ni/MgO/CeZrO
Effect of P_{CO2}			
α, CH_4	0.79	–0.87	0
α, CO_2	1.90	0.53	0.98
Effect of P_{H2O}			
β, CH_4	–0.06	–0.64	0.03
β, CO_2	–1.57	–2.59	–1.08
Apparent activation energy, E_{app} (kJ/mol)			
CO_2	247.0	160.1	165.7
CH_4	69.1	219.6	67.4

Table 18.6 Tri-reforming of methane mechanistic steps for LHHW model proposed by Song and Pan (2004)

Elementary steps	Kinetic model
Adsorption of reactants $CH_4 + S \overset{K_1}{\leftrightarrow} CH_4 - S$ $CO_2 + S \overset{K_2}{\leftrightarrow} CO_2 - S$	$-r_{CH_4} = \frac{kK_1K_2P_{CH_4}P_{CO_2}}{\left(1+K_1P_{CH_4}+K_2P_{CO_2}\right)^2}$
Reaction on catalysts surface $CH_4 - S + CO_2 - S \overset{k}{\rightarrow} 2H_2 + 2CO + 2S(RDS)$	

Note: k and S represent the rate constant and accessible active sites, respectively

Table 18.7 Kinetic expressions and estimated parameters for steam reforming, dry reforming, and water-gas shift reaction side reactions of tri-reforming of methane (García-Vargas et al. 2015a)

Reactions	Kinetic parameters	Kinetic models
Steam reforming of methane (SRM)	$E_{a_1} = 74.7$ kJ/mol $k_1^0 = 85.8$ mol s^{-1} kPa^{-1}	$r_{SRM} = k_1P_{CH_4}\left(1-\frac{P_{H_2}^3P_{CO}}{K_{SRM}P_{CH_4}P_{H_2O}}\right)$ $K_{SRM} = 1.198\times10^{17}e^{\left(\frac{-26830}{T}\right)}$
Dry reforming of methane (DRM)	$E_{a_2} = 77.8$ kJ/mol $k_2^0 = 71.0$ mol s^{-1} kPa^{-1}	$r_{DRM} = k_2P_{CH_4}\left(1-\frac{P_{H_2}^2P_{CO}^2}{K_{DRM}P_{CH_4}P_{H_2O}}\right)$ $K_{DRM} = 6.780\times10^{18}e^{\left(\frac{-31230}{T}\right)}$
Water-gas shift reaction (WGS)	$E_{a_3} = 54.3$ kJ/mol $k_3^0 = 149.9$ mol s^{-1} kPa^{-1}	$r_{WGS} = k_3\left(\frac{P_{H_2O}P_{CO}}{P_{H_2}}-\frac{P_{CO_2}}{K_{WGS}}\right)$ $K_{WGS} = 10^{\left(\frac{2078}{T}-2.029\right)}$

reforming, and water-gas shift reaction is 74.7, 77.8, and 54.3 kJ/mol, respectively, and the kinetic models show a relatively good fitness to experimental data with mean deviations from 10.8% to 19.4%.

Unlike the kinetic expressions suggested by García-Vargas et al. (2015a), Chein et al. (2017) proposed that different kinetic rate models involved steam reforming, reverse CO_2 methanation (RCM), and water-gas shift reaction (Table 18.8) since they found that the presence of H_2O induced a great influence on tri-reforming reaction rate in their parametric investigation. They also reported that in the absence of water,

Table 18.8 Kinetic rate models for steam reforming, reverse CO_2 methanation, and water-gas shift reactions in tri-reforming of methane (Chein et al. 2017)

Reactions	Kinetic rate models
Steam reforming of methane (SRM)	$r_{SRM} = \frac{\frac{k_1}{P_{H_2}^{2.5}}\left(P_{CH_4}P_{H_2O} - \frac{P_{H_2}^3 P_{CO}}{K_{SRM}}\right)}{DEN^2}$ $K_{SRM} = 1.198\times10^{23} e^{\left(\frac{-26830}{T}\right)}$ $k_1 = 3.711\times10^{17} e^{\left(\frac{-240100}{RT}\right)}$ $DEN = 1 + K_{CH_4}P_{CH_4} + K_{CO}P_{CO} + K_{H_2}P_{H_2} + \frac{K_{H_2O}P_{H_2O}}{P_{H_2}}$
Water-gas shift reaction (WGS)	$r_{WGS} = \frac{\frac{k_2}{P_{H_2}}\left(P_{H_2O}P_{CO} - \frac{P_{H_2}P_{CO_2}}{K_{WGS}}\right)}{DEN^2}$ $K_{WGS} = 1.767\times10^{-2} e^{\left(\frac{4400}{T}\right)}$ $k_2 = 5.431 e^{\left(\frac{-67130}{RT}\right)}$
Reverse CO_2 methanation (RCM)	$r_{RCM} = \frac{\frac{k_3}{P_{H_2}^{3.5}}\left(P_{CH_4}P_{H_2O}^2 - \frac{P_{H_2}^4 P_{CO_2}}{K_{RCM}}\right)}{DEN^2}$ $K_{RCM} = K_{SRM}K_{WGS}$ $k_3 = 8.96\times10^{16} e^{\left(\frac{-24390}{RT}\right)}$

Note: Denominator *DEN*

dry reforming of methane became the predominant reaction inducing a low H_2/CO ratio of 1, while steam reforming of CH_4 was the main reaction with the absence of CO_2 reactant.

As partial conclusion, this section presents a comprehensive review on various kinetic models derived from the respective rate-determining step in association with different proposed mechanistic steps. Many kinetic models were widely reported into three forms, namely power law, ER, and LHHW models. The power law models could provide empirical reaction orders to reveal the dependence of reaction activity

on reactant partial pressure. However, it could not reflect the essential influence factor of rate-determining step toward catalytic activity with respect to mechanistic pathway. Thus, numerous rate-determining steps presented in LHHW and ER models have been suggested for predicting the consumption rate of reactants. Generally, these rate-determining steps involve C–H bonds cleavage in CH_4 molecule on metal, dissociation of oxidizing agent (e.g., O_2, CO_2, or H_2O) on metal or support, formation of intermediate species and decomposition, oxidation of carbonaceous species, and several other parallel reactions. To implement the dry reforming and tri-reforming technologies for industrial application, the best-fit kinetic modeling associated with the intrinsic dry reforming and tri-reforming mechanism is indispensable for efficiently designing the catalyst system and optimizing the reactor design.

18.7 Industrial Applications

Despite the interest in scaling up this technology, problems related to catalyst activity and stability still need to be solved to advance the readiness level of this process. To the best of our knowledge, only very few reports are available on the literature regarding the scale-up of dry reforming of methane. Rego de Vasconcelos and Lavoie (2018) recently reported the scale-up of a dry reforming technology combined with renewable electricity. In this case, an electrified fixed-bed reactor is used in combination with steel wool as a catalyst. The tests performed showed CH_4 and CO_2 conversions equal to 100% over 200 h of time on stream. The advantages of this approach are the very low cost and the good catalytic performance of the catalyst as well as the use of renewable electricity to provide the energy to the reaction. The technology evolved from bench scale with capacity of treating less than 1 L/min of a mixture containing CH_4 and CO_2 to a pilot capable of treating 40 L/min of the same gaseous mixture. The technology developed is compatible for biogas, tail gas, and natural gas.

The Linde Group has also claimed the development of an innovative dry reforming process that convert large volumes of CO_2 into syngas using a nickel-based catalyst, which has been tested for more than 1000 h (Linde 2019). Besides CH_4 and CO_2, water is also used in this process to prevent catalyst deactivation by coke formation (Tullo 2016). The Linde Pilot Reformer research facility is located at Pullach (Germany) and is currently under scale up for commercial application.

Steam reforming of natural gas has been deployed at large industrial scale. This technology can be transposed to the reforming of landfill gas, as the case of the VABHYOGAZ3 project, financed by ADEME in France (ADEME 2016). This project aims to design a complete production chain of liquid hydrogen production from landfill gas containing up to 60% of CH_4. Landfill gas is firstly reformed into syngas at around 900 °C, with a large excess of steam (molar ratio of steam/methane of around 4:1). In fact, the landfill gas used in this project containing CH_4, CO_2, and O_2 is fed together with steam to the reforming catalytic reactor. The syngas is then converted into a mixture rich in H_2 and CO_2 by water-gas shift reaction. Pure hydrogen (99.99%) is obtained by the pressure swing adsorption process, which is then

compressed to 350–700 bar into liquid hydrogen for injection in hydrogen-fueled vehicles. CO_2 obtained from the pressure swing adsorption process is valorized by producing sodium bicarbonate for flue gas treatment. The current production unit developed by the industrial partners of this project has a capacity of 10 kg of liquid hydrogen per day (ADEME 2016; Pham Minh et al. 2018a, b). The consortium of this project can deploy production units of 80–800 kg of liquid hydrogen per day from landfill gas with competitive cost of liquid hydrogen versus other production ways (e.g., electrolysis of water).

18.8 Conclusions

Biogas production from biological degradation of biomass and biowaste continuously increases worldwide. Heat and electricity production from biogas have been largely deployed. Current research and development on biogas valorization mostly consists in the production of value-added chemicals via biogas reforming. Both dry- and tri-reforming processes need high temperature (e.g., 800–1000 °C) and low pressure (e.g., atmospheric pressure) to reach high methane conversion. The utilization of a performing catalyst is indispensable to obtain exploitable reaction rate and good syngas selectivity. The main criteria of such a catalyst include high thermal stability, high coke resistance, high activity, and stability. Nickel is the most appropriate active metal for biogas reforming, while various supports have been found suitable. Significant efforts have also been devoted to kinetic and mechanism studies of dry- and tri-reforming processes. This is mandatory for reactor design for further deployment of these processes at large-scale.

References

Abdoulmoumine N, Adhikari S, Kulkarni A, Chattanathan, S (2015) A review on biomass gasification syngas cleanup. Appl. Ener. 155:294-307.

Abdullah B, Ghani NAA, Vo DVN (2017) Recent advances in dry reforming of methane over Ni-based catalysts. J Clean Prod 162:170–185

Abdulrasheed A, Jail A, Gambo Y, Ibrahim M, Hambali H, Hamid M (2019) A review on catalyst development for dry reforming of methane to syngas: recent advances. Renew Sust Energ Rev 108:175–193

Achinas S, Achinas V, Euverink GJW (2017) A technological overview of biogas production from biowaste. Engineering 3:299–307

ADEME (2016) Vabhyogaz 3—Valorisation du biogaz en hydrogène. https://occitanie.ademe.fr/sites/default/files/valorisation-biogaz-hydrogene-vabhyogaz.pdf. Accessed 17 May 2019

Amin MH, Patel J, Sage V, Lee WJ, Periasamy S, Dumbre D, Mozammel T, Prasad V, Samanta C, Bhargava SK (2015) Tri-reforming of methane for the production of syngas: review on the process, catalyst and kinetic mechanism. APCChE 2015 congress incorporating Chemeca, no. Sept: 1–10

Anchieta CG, Assaf EM, Assaf JM (2019) Effect of ionic liquid in Ni/ZrO_2 catalysts applied to syngas production by methane tri-reforming. Int J Hydrogen Energ 44:9316–9327

Angelidaki I, Treu L, Tsapekos P, Luo G, Campanaro S, Wenzel H, Kougias PG (2018) Biogas upgrading and utilization: current status and perspectives. Biotechnol Adv 36:452–466

Aramouni NAK, Touma JG, Tarboush BA, Zeaiter J, Ahmad MN (2018) Catalyst design for dry reforming of methane: analysis review. Renew Sust Energ Rev 82:2570–2585

Asimakopoulos K, Gavala, HN, Skiadas IV (2018) Reactor systems for syngas fermentation processes: A review. Chem. Eng. J. 348:732–744.

Aw MS, Črnivec IGO, Pintar A (2014a) Tunable ceria–zirconia support for nickel–cobalt catalyst in the enhancement of methane dry reforming with carbon dioxide. Catal Commun 52:10–15

Aw MS, Črnivec IGO, Djinovic P, Pintar A (2014b) Strategies to enhance dry reforming of methane: synthesis of ceria-zirconia/nickelecobalt catalysts by freeze-drying and NO calcination. Int J Hydrogen Energ 39:12636–12647

Aw MS, Zorko M, Djinovic P, Pintar A (2015) Insights into durable NiCo catalysts on β-SiC/$CeZrO_2$ an γ-Al_2O_3/$CeZrO_2$ advanced supports prepared from facile methods for CH_4–CO_2 dry reforming. Appl Catal B 164:100–112

Ayodele BV, Khan MR, Lam SS, Cheng CK (2016) Production of CO-rich hydrogen from methane dry reforming over lanthania-supported cobalt catalyst: kinetic and mechanistic studies. Int J Hydrogen Energ 41:4603–4615

Aziz NIHA, Hanafiah MM, Gheewala SH (2019) A review on life cycle assessment of biogas production: challenges and future perspectives in Malaysia. Biomass Bioenergy 122:361–374

Bao Z, Lu Y, Yu F (2017) Kinetic study of methane reforming with carbon dioxide over NiCeMgAl bimodal pore catalyst. AICHE J 63:2019–2029

Bian Z, Das S, Wai MH, Hongmanorom P, Kawi S (2017) A review on bimetallic nickel-based catalysts for CO_2 reforming of methane. ChemPhysChem 18:3117–3134

Biogas Renewable Energy (2019). http://www.biogas-renewable-energy.info/biogas_composition.html. Accessed 8 May 2019

Bobadilla LF, Garcilaso V, Centeno MA, Odriozola JA (2017) Monitoring the reaction mechanism in model biogas reforming by in situ transient and steady-state DRIFTS measurements. ChemSusChem 10:1193–1201

Boukha Z, Kacimi M, Pereira MFR, Faria JL, Figueiredo JL, Ziyad M (2007) Methane dry reforming on Ni loaded hydroxyapatite and fluoroapatite. Appl Catal A Gen 317:299–309

Boukha Z, Yeste MP, Cauqui MA, González-Velasco JR (2019) Influence of Ca/P ratio on the catalytic performance of Ni/hydroxyapatite samples in dry reforming of methane. Appl Catal A Gen 580:34–45

Brown RC (2011) Thermochemical processing of biomass: conversion into fuels, chemicals and power. Wiley, Chichester, UK

Cao P, Adegbite S, Zhao H, Lester E, Wu T (2018) Tuning dry reforming of methane for F-T syntheses: a thermodynamic approach. Appl Energy 227:190–197

Chein RY, Hsu WH (2018) Thermodynamic analysis of syngas production via tri-reforming of methane and carbon gasification using flue gas from coal-fired power plants. J Clean Prod 200:242–258

Chein RY, Wang CY, Yu CT (2017) Parametric study on catalytic tri-reforming of methane for syngas production. Energy 118:1–17

Clemens H, Bailis R, Nyambane A, Ndung'u V (2018) Africa biogas partnership program: a review of clean cooking implementation through market development in East Africa. Energ Sust Develop 46:23–31

Cui Y, Zhang H, Xu H, Li W (2007) Kinetic study of the catalytic reforming of CH_4 with CO_2 to syngas over Ni/α-Al_2O_3 catalyst: the effect of temperature on the reforming mechanism. Appl Catal A Gen 318:79–88

Das S, Sengupta M, Bag A, Shah M, Bordoloi A (2018) Facile synthesis of highly disperse Ni–co nanoparticles over mesoporous silica for enhanced methane dry reforming. Nanoscale 10:6409–6425

Daza CE, Gallego J, Mondragón F, Moreno S, Molina R (2010) High stability of Ce-promoted Ni/mg-Al catalysts derived from hydrotalcites in dry reforming of methane. Fuel 89:592–603

Dębek R, Zubek K, Motak M, Galvez ME, Da Costa P, Grzybek T (2015) Ni–Al hydrotalcite-like material as the catalyst precursors for the dry reforming of methane at low temperature. C R Chim 18:1205–1210

Di Maio R, Fais S, Ligas P, Piegari E, Raga R, Cossu R (2018) 3D geophysical imaging for site-specific characterization plan of an old landfill. Waste Manag 76:629–642
Diez-Ramirez J, Dorado F, Martinez-Valiente A, Garcia-Vargas J, Sanchez P (2016) Kinetic, energetic and exergetic approach to the methane tri-reforming process. Int J Hydrogen Energ 41:19339–19348
Djinovic P, Pintar A (2017) Stable and selective syngas production from dry CH_4-CO_2 streamsover supported bimetallic transition metal catalysts. Appl Catal B 206:675–682
Djinovic P, Crnivec IGO, Erjavec B, Pintar A (2012) Influence of active metal loading and oxygen mobility on coke-free dry reforming of Ni–co bimetallic catalysts. Appl Catal B 125:259–270
Djinovic P, Crnivec IGO, Pintar A (2015) Biogas to syngas conversion without carbonaceous deposits via thedry reforming reaction using transition metal catalysts. Catal Today 253:155–162
Eklund B, Anderson EP, Walker BL, Burrows DB (1998) Characterization of landfill gas composition at the fresh kills municipal solid-waste landfill. Environ Sci Technol 32:2233–2237
Elfattah S, Eldrainy Y, Attia A (2016) Upgrade Egyptian biogas to meet the natural gas network quality standard. Alexandria Eng J 55:2279–2283
Estephane J, Aouad S, Hany S, El Khoury B, Gennequin C, El Zakhem H, El Nakat J, Aboukaïs A, Aad EA (2015) CO_2 reforming of methane over Ni–CO/ZSM5 catalysts. Aging and carbon deposition study. Int J Hydrogen Energ 40:9201–9208
Faungnawakij K, Kikuchi R, Eguchi K (2007) Thermodynamic analysis of carbon formation boundary and reforming performance for steam reforming of dimethyl ether. J Power Sources 164:73–79
García-Vargas JM, Valverde JL, Dorado F, Sanchez P (2014a) Influence of the support on the catalytic behaviour of Ni catalysts for the dry reforming reaction and the tri-reforming process. J Mol Catal A Chem 395:108–116
García-Vargas JM, Valverde JS, Díez J, Sánchez P, Dorado F (2014b) Influence of alkaline and alkaline-earth cocations on the performance of Ni/β-SiC catalysts in the methane tri-reforming reaction. Appl Catal B 148–149:322–329
García-Vargas JM, Valverde JL, Díez J, Dorado F, Sánchez P (2015a) Catalytic and kinetic analysis of the methane tri-reforming over a Ni–mg/β-SiC catalyst. Int J Hydrogen Energ 40:8677–8687
García-Vargas JM, Valverde JS, Díez J, Sánchez P, Dorado F (2015b) Preparation of Ni–mg/β-SiC catalysts for the methane tri-reforming: effect of the order of metal impregnation. Appl Catal B 164:316–323
Goula MA, Charisiou ND, Papageridis KN, Delimitis A, Pachatouridou E, Iliopoulou EF (2015) Nickel on alumina catalysts for the production of hydrogen rich mixtures via the biogas dry reforming reaction: influence of the synthesis method. Int J Hydrogen Energ 40:9183–9200
GRDF, Gaz Réseau Distribution France (2019). https://www.grdf.fr/dossiers/biomethane-biogaz/unites-injection-gaz-vert-biomethane-reseau. Accessed 11 May 2019
Grouset D, Ridart C (2018) Lowering energy spending together with compression, storage, and transportation costs for hydrogen distribution in the early market. In: Azzaro-Pantel C (ed) Hydrogen supply chains-design, deployment and operation. Academic Press, Waltham, MA, pp 207–270
Guharoy U, Le Saché E, Cai Q, Reina TR, Gu S (2018) Understanding the role of Ni-Sn interaction to design highly effective CO_2 conversion catalysts for dry reforming of methane. J CO2 Util 27:1–10
Hoo PY, Hashim H, Ho WS (2018) Opportunities and challenges: landfill gas to biomethane injection into natural gas distribution grid through pipeline. J Clean Prod 175:409–419
Horn R, Schlögl R (2015) Methane activation by heterogeneous catalysis. Catal Lett 145:23–39
Hou Z, Chen P, Fang H, Zheng X, Yashima T (2006) Production of synthesis gas via methane reforming with CO_2 on noble metals and small amount of noble-(Rh-) promoted Ni catalysts. Int J Hydrogen Energ 31:555–561
IRENA (2017) International Renewable Energy Agency: Renew Capacity Statistics 2016
Jafarbegloo M, Tarlani A, Mesbah AW, Sahebdelfar S (2015) Thermodynamic analysis of carbon dioxide reforming of methane and its practical relevance. Int J Hydrogen Energ 40:2445–2451

Jaffrin A, Bentounes N, Joan A, Makhlouf S (2003) Landfill biogas for heating greenhouses and providing carbon dioxide supplement for plant growth. Biosyst Eng 86:113–123

Jang WJ, Shim JO, Kim HM, Yoo SY, Roh HS (2019) A review on dry reforming of methane in aspect of catalytic properties. Catal Today 324:15–26

Jiang H, Li H, Xu H, Zhang Y (2007) Preparation of $Ni/Mg_xTi_{1-x}O$ catalysts and investigation on their stability in tri-reforming of methane. Fuel Process Technol 88:988–995

Jiang S, Lu Y, Wang S, Zhao Y, Ma X (2017) Insight into the reaction mechanism of CO_2 activation for CH_4 reforming over NiO-MgO: a combination of DRIFTS and DFT study. Appl Surf Sci 416:59–68

Kaparaju P, Rintala J (2013) Generation of heat and power from biogas for stationary applications: boilers, gas engines and turbines, combined heat and power (CHP) plants and fuel cells. In: Wellinger A, Murphy J, Baxter D (eds) The biogas handbook, science, production and applications. Woodhead Publishing, Oxford, Cambridge, Philadelphia, New Delhi, pp 404–427

Karam L, Hassan NE (2018) Advantages of mesoporous silica based catalysts in methane reforming by CO_2 from kinetic perspective. J Env Chem Eng 6:4289–4297

Kawi S, Kathiraser Y, Ni J, Oemar U, Li Z, Saw ET (2015) Progress in synthesis of highly active and stable nickel-based catalysts for carbon dioxide reforming of methane. ChemSusChem 8:3556–3575

Kaza S, Yao L, Bhada-Tata P, Van Woerden F (2018) What a waste 2.0: a global snapshot of solid waste management to 2050. The World Bank, Washington, DC

Khalil M, Berawi MA, Heryanto R, Rizalie A (2019) Waste to energy technology: the potential of sustainable biogas production from animal waste in Indonesia. Renew Sust Energ Rev 105:323–331

Khan IU, Othman MHD, Hashima H, Matsuura T, Ismail AF, Rezaei-DashtArzhandi M, Wan Azelee I (2017) Biogas as a renewable energy fuel—a review of biogas upgrading, utilization and storage. Energy Convers Manag 150:277–294

Kroll VCH, Swaan HM, Lacombe S, Mirodatos C (1997) Methane reforming reaction with carbon dioxide over Ni/SiO_2 catalyst. J Catal 398:387–398

Kumar R, Kumar K, Choudary NV, Pant KK (2019) Effect of support materials on the performance of Ni-based catalysts in tri-reforming of methane. Fuel Process Technol 186:40–52

Kvist T, Aryal N (2019) Methane loss from commercially operating biogas upgrading plants. Waste Manag 87:295–300

Linde (2019) "Innovative Dry Reforming Process." https://www.linde-engineering.com/en/innovations/innovate-dry-reforming/index.html. Accessed 15 May 2019

Lino AVP, Calderon YNC, Mastelaro VR, Assaf EM, Assaf JM (2019) Syngas for Fischer-Tropsch synthesis by methane tri-reforming using nickel supported on $MgAl_2O_4$ promoted with Zr, Ce and Ce-Zr. Appl Surf Sci 481:747–760

Liu K, Song C, Subramani V (2010) Hydrogen and syngas production and purification technologies. Wiley, Hoboken, USA

Majewski AJ, Wood J (2014) Tri-reforming of methane over $Ni@SiO_2$ catalyst. Int J Hydrogen Energ 39:12578–12585

Mittal S, Ahlgren EO, Shukla PR (2018) Barriers to biogas dissemination in India: a review. Energy Policy 112:361–370

Mo W, Ma F, Liu Y, Liu J, Zhong M, Nulahong A (2015) Preparation of porous Al_2O_3 by template method and its application in Ni-based catalyst for CH_4/CO_2 reforming to produce syngas. Int J Hydrogen Energ 40:16147–16158

Mohamedali M, Henni A, Ibrahim H (2018) Recent advances in supported metal catalysts for syngas production from methane. ChemEng 2:9

Mudhoo A (2012) Biogas production: pretreatment methods in anaerobic digestion. Wiley/Scrivener Publishing LLC, Hoboken, NJ/Salem, MA

Nanda S, Li K, Abatzoglou N, Dalai AK, Kozinski JA (2017) Advancements and confinements in hydrogen production technologies. In: Dalena F, Basile A, Rossi C (eds) Bioenergy systems for the future. Woodhead Publishing, Sawston, UK, pp 373–418

Néron A, Lantagne G, Marcos B (2012) Computation of complex and constrained equilibria by minimization of the Gibbs free energy. Chem Eng Sci 82:260–271

Nikoo MK, Amin NAS (2011) Thermodynamic analysis of carbon dioxide reforming of methane in view of solid carbon formation. Fuel Process Technol 92:678–691

Okonkwo C, Onokpite E, Onokwai A (2018) Comparative study of the optimal ratio of biogas production for, various organic wastes and weeds for digester/restarted digester. J King Saud Univ-Eng Sci 30:123–129

Osazuwa OU, Setiabudi HD, Abdullah S, Cheng CK (2017) Syngas production from methane dry reforming over $SmCoO_3$ perovskite catalyst: kinetics and mechanistic studies. Int J Hydrogen Energ 42:9707–9721

Pakhare D, Spivey J (2014) A review of dry (CO_2) reforming of methane over noble metal catalysts. Chem Soc Rev 43:7813–7837

Pakhare D, Schwartz V, Abdelsayed V, Haynes D, Shekhawat D, Poston J, Spivey J (2014) Kinetic and mechanistic study of dry (CO_2) reforming of methane over Rh-substituted $La_2Zr_2O_7$ pyrochlores. J Catal 316:78–92

Papadopoulou C, Matralis H, Verykios X (2012) Utilization of biogas as a renewable carbon source: dry reforming of methane. In: Guczi L, Erdôhelyi A (eds) Catalysis for alternative energy generation. Springer Nature, New York, NY, pp 57–127

Persson M, Jönsson O, Wellinger A (2009) IEA Bioenergy, Task 37—Energy from biogas and landfill gas

Pertiwiningrum A, Agus DKC, Wuri MA (2018) Renewable energy of biogas through integrated organic cycle system in tropical system. In: Gokten S, Kucukkocaoglu G (eds) Energy management for sustainable development. IntechOpen, London, UK, pp 99–117

Pham Minh D, Phan TS, Grouset D, Nzihou A (2018a) Thermodynamic equilibrium study of methane reforming with carbon dioxide, water and oxygen. J Clean Energ Technol 6:309–313

Pham Minh D, Siang TJ, Vo DVN, Phan TS, Ridart C, Nzihou A, Grouset D (2018b) Hydrogen production from biogas reforming: an overview of steam reforming, dry reforming, dual reforming, and tri-reforming of methane. In: Hydrogen supply chains. Elsevier, Amsterdam, pp 111–166

Phan TS, Sane AR, Rego de Vasconcelos B, Nzihou A, Sharrock P, Grouset D, Minh DP (2018) Hydroxyapatite supported bimetallic cobalt and nickel catalysts for syngas production from dry reforming of methane. Appl Catal B 224:310–321

Pino L, Vita A, Cipitì F, Laganà M, Recupero V (2011) Hydrogen production by methane tri-reforming process over Ni–ceria catalysts: effect of La-doping. Appl Catal B 104:64–73

Pradhan BB, Limmeechokchai L (2017) Electric and biogas stoves as options for cooking in Nepal and Thailand. Energy Procedia 138:470–475

Puigjaner L (2011) Syngas from waste emerging technologies. Springer, New York, NY

Pullen T (2015) Anaerobic digestion- making biogas-making energy. Routledge, New York, NY

Rahnama H, Farniaei M, Abbasi M, Rahimpour MR (2014) Modeling of synthesis gas and hydrogen production in a thermally coupling of steam and tri-reforming of methane with membranes. J Ind Eng Chem 20:1779–1792

Rego de Vasconcelos BR (2016) Phosphates-based catalyst for synthetic gas (syngas) production using CO_2 and CH_4. Ph.D. thesis, Ecole Nationale Supérieure des Mines d'Albi-Carmaux, Albi, France

Rego de Vasconcelos B, Lavoie JM (2018) Is dry reforming the solution to reduce natural gas carbon footprint? Int J Ener Prod Manag 3:44–56

Rego de Vasconcelos B, Pham Minh D, Lyczko N, Phan TS, Sharrock P, Nzihou A (2018a) Upgrading greenhouse gases (methane and carbon dioxide) into syngas using nickel-based catalysts. Fuel 226:195–203

Rego de Vasconcelos BR, Pham Minh D, Sharrock P, Nzihou A (2018c) Regeneration study of Ni/hydroxyapatite spent catalyst from dry reforming. Catal Today 310:107–115

Rostrup-Nielsen JR, Hansen JHB (1993) CO_2 reforming of methane over transition metals. J Catal 144:38–49

Sahota S, Shaha G, Ghosha P, Kapoor R, Sengupta S, Singh P, Vijay V, Sahay A, Vijay VK, Thakur IS (2018) Review of trends in biogas upgradation technologies and future perspectives. Biores Technol Rep 1:79–88

San José-Alonso D, Illán-Gómez MJ, Román-Martínez MC (2011) K and Sr promoted co alumina supported catalysts for the CO_2 reforming of methane. Catal Today 176:187–190

Sapountzi FM, Zhao C, Boréave A, Retailleau-Mevel L, Niakolas D, Neofytidis C, Vernoux P (2018) Sulphur tolerance of au-modified Ni/GDC during catalytic methane steam reforming. Cat Sci Technol 8:1578–1588

Scarlat N, Dallemand JF, Fahl F (2018) Biogas: developments and perspectives in Europe. Renew Energy 129:457–472

Schildhauer TJ, Biollaz MA (2016) Synthetic natural gas from coal, dry biomass, and power-to-gas applications. Wiley, Hoboken, NJ

Shah YT (2017) Chemical energy from natural gas and synthetic gas. CRC Press, Boca Raton, FL

Si LJ, Wang CZ, Sun NN, Wen X, Zhao N, Xiao FK, Wei W, Sun YH (2012) Influence of preparation conditions on the performance of Ni-CaO-ZrO_2 catalysts in the tri-reforming of methane. J Fuel Chem Technol 40:210–215

Singh SA, Madras G (2016) Sonochemical synthesis of Pt, Ru doped TiO_2 for methane reforming. Appl Catal A Gen 518:102–114

Singha RK, Shukla A, Yadav A, Adak S, Iqbal Z, Siddiqui N, Bal R (2016) Energy efficient methane tri-reforming for synthesis gas production over highly coke resistant nanocrystalline Ni–ZrO_2 catalyst. Appl Energy 178(2016):110–125

Song C, Pan W (2004) Tri-reforming of methane: a novel concept for catalytic production of industrially useful synthesis gas with desired H_2/CO ratios. Catal Today 98:463–484

Tang P, Zhu Q, Wu Z, Ma D (2014) Methane activation: the past and future. Energy Environ Sci 7:2580–2591

Themelis N, Ulloa P (2007) Methane generation in landfills. Renew Energy 32:1243–1257

Tullo AH (2016) Dry reforming puts CO_2 to work. Chem Eng News 94:30. https://cen.acs.org/content/cen/articles/94/i17/Dry-reforming-puts-CO2-work.html. Accessed 17 May 2019

Wang S, Lu GQM (1996) Carbon dioxide reforming of methane to produce synthesis gas over metal-supported catalysts: state of the art. Energ Fuels 10:896–904

Wei J, Iglesia E (2004) Isotopic and kinetic assessment of the mechanism of reactions of CH_4 with CO_2 or H_2O to form synthesis gas and carbon on nickel catalysts. J Catal 224:370–383

Weiland P (2010) Biogas production: current state and perspectives. Appl Microbiol Biotechnol 85:849–860

Wolfbeisser A, Sophiphun O, Bernardi J, Wittayakun J, Föttinger K, Rupprechter G (2016) Methane dry reforming over ceria-zirconia supported Ni catalysts. Catal Today 277:234–245

Xu J, Zhou W, Li Z, Wang J, Ma J (2009) Biogas reforming for hydrogen production over nickel and cobalt bimetallic catalysts. Int J Hydrogen Energ 34:6646–6654

Yasmin N, Grundmann P (2019) Adoption and diffusion of renewable energy—the case of biogas as alternative fuel for cooking in Pakistan. Renew Sust Energ Rev 101:255–264

Youcai Z, Ziyang L (2017) General structure of sanitary landfill. In: Pollution control and resource recovery: municipal solid wastes at landfill. Elsevier, Amsterdam, pp 1–10

Zhou H, Zhang T, Sui Z, Zhu YA, Han C, Zhu K, Zhou X (2018) A single source method to generate Ru-Ni-MgO catalysts for methane dry reforming and the kinetic effect of Ru on carbon deposition and gasification. Appl Catal B 233:143–159